npj | breast cancer

Article

Published in partnership with the Breast Cancer Research Foundation

https://doi.org/10.1038/s41523-026-00916-1

Transcriptomic analysis to uncover the mechanism of radiosensitization of AR-positive triple-negative breast cancers with AR inhibition

Breanna McBean[1,2,3,7], Benjamin Hauk[4,7], Anna R. Michmerhuizen[1,7], Benjamin C. Chandler[1], Andrea M. Pesch[1], Lynn M. Lerner[1], Douglas Gurdak[4,5], Connor Ward[1], Priyanka Rana[4,5], Reine Abou Zeidane[4,5], Vesna Mercer[4,5], Mingfang Tao[4,5], Ethan Hochmuth[4,5], Kassidy M. Jungles[1], Stephanie The[1], Meilan Liu[1], Daniel E. Spratt[4,5], Alan P. Boyle[2,3], Lori J. Pierce[1] & Corey W. Speers[4,5,6] ✉

The androgen receptor (AR) has been identified as a driver of tumor growth and radioresistance in triple-negative breast cancers (TNBC), though the mechanistic role of AR in response to radiation therapy (RT) remains unknown. Here, we demonstrate that inhibition with the second-generation anti-androgen, apalutamide, but not darolutamide, is sufficient to radiosensitize AR+ TNBC models (rER: 1.34-1.41; rER: 0.96-1.11, respectively). Cells with low AR expression were not radiosensitized by AR inhibition (rER: 0.96-1.03). Mechanistically, while stimulation with the AR-agonist R1881 is sufficient to induce nuclear translocation of AR in AR+ TNBC cells, AR inhibition with enzalutamide, apalutamide, or darolutamide blocked AR nuclear translocation. When cells are treated with R1881+RT, nuclear translocation of AR was induced at similar or greater levels compared to R1881 alone in AR+ TNBC cells. Combination treatment of RT with enzalutamide reduced nuclear localization of AR (32-39% reduction) compared to RT alone. Transcriptional evaluation with RNA-Seq after AR stimulation and RT demonstrated changes in the MAPK/ERK signaling pathway, among others. Overexpression of ERK reduces the radiosensitizing ability of second-generation anti-androgens, suggesting that AR-mediated radioresistance may be due, at least in part, to downstream MAPK/ERK signaling. These findings suggest that AR-mediated radioresistance is at least partially due to downstream MAPK/ERK signaling. Together this work builds on the mechanistic understanding of AR-mediated radioresistance in AR+ TNBC which may expose vulnerabilities in resistance to combination treatment with AR inhibition and RT.

Therapies targeting the androgen receptor (AR) have been of increasing interest for the treatment of AR-positive (AR+) breast tumors, including AR+ triple negative breast cancers (TNBC)[1–5]. Due to the ineffectiveness of molecular targeted therapies, patients with TNBC generally receive multi-modal treatments including surgery, chemotherapy, and radiation therapy (RT). Recent work has demonstrated that therapies targeting the AR may be effective for the treatment of AR+ TNBC as monotherapy[6–8]. Additional work indicates that AR inhibitors, when combined with RT, result in significant radiosensitization in AR+ TNBC models[9–11], but may have different effects in tumors expressing both AR and ER together[12–14].

While many anti-androgen therapies have been investigated for the treatment of AR+ cancers, including AR+ breast cancer[2], here we focus

[1]Department of Radiation Oncology, University of Michigan, Ann Arbor, MI, USA. [2]Department of Human Genetics, University of Michigan, Ann Arbor, MI, USA. [3]Department of Computational Medicine and Bioinformatics, University of Michigan, Ann Arbor, MI, USA. [4]University Hospitals Seidman Cancer Center and Case Western Reserve University, Cleveland, OH, USA. [5]Case Comprehensive Cancer Center, Cleveland, OH, USA. [6]Department of Radiation Oncology, University of Alabama, Birmingham, Birmingham, AL, UK. [7]These authors contributed equally: Breanna McBean, Benjamin Hauk, Anna R. Michmerhuizen. ✉e-mail: cspeers@uabmc.edu

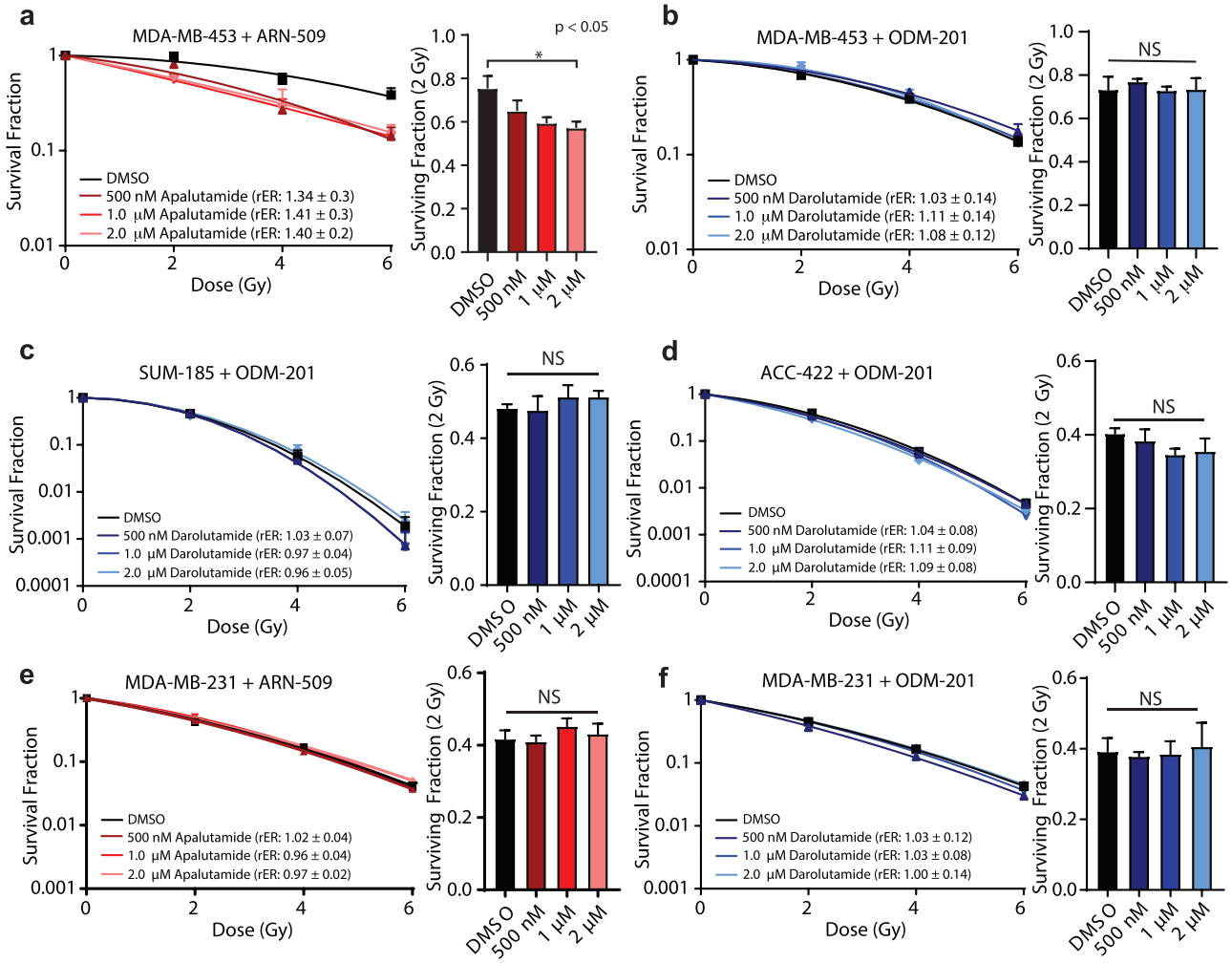

Fig. 1 | AR inhibition with apalutamide but not darolutamide radiosensitizes AR + TNBC but not AR- TNBC models. One-hour pretreatment with (**a**) apalutamide (ARN-509) but not (**b**) darolutamide (ODM-201) is sufficient to radiosensitize AR+ TNBC MDA-MB-453 cells. One-hour pretreatment with darolutamide also does not radiosensitize AR+ (**c**) SUM-185 cells (**d**) and ACC-422 cells. Radiosensitization with (**e**) apalutamide and (**f**) darolutamide was assessed in MDA-MB-231 cells with low AR expression. Experiments were performed in triplicate and graphed as mean ± SEM. * $p < 0.05$, NS = not significant, AR: androgen receptor, TNBC: triple-negative breast cancer, SEM: Standard error of the mean.

on the second-generation anti-androgens and their effect on radiation response in TNBC[7,15]. While AR inhibition and knockdown have previously been demonstrated to sensitize AR+ models, including prostate cancer[16–18], glioblastoma[19], and breast cancer[9–11], to RT both in vitro and in vivo, the mechanism of radiosensitization and the role of AR in driving resistance to radiotherapy in AR+ TNBC remains understudied and of clinical importance. Previously, we and others have demonstrated that second generation anti-androgens can sensitize AR+ TNBC models to radiation treatment[9–11]. Here we sought to expand previous studies by exploring the utility of second-generation anti-androgens in AR high- and low-expressing TNBC models, as well as investigating AR-mediated genomic mechanisms of radioresistance. Notably, as AR is increasingly being investigated as a target for therapy, there remains a critical need for the development of accurate biomarkers of response to AR inhibitors to correctly identify the patient populations that will most reliably respond to AR targeted therapies.

Results

AR inhibition with apalutamide, but not darolutamide, radiosensitizes AR+ TNBC models

Having previously observed radiosensitization of AR+ TNBC cells with AR knockdown[10] or pharmacologic inhibition[9,20], we wanted to know if inhibition of AR using the second-generation anti-androgens apalutamide or darolutamide was sufficient to radiosensitize AR+ TNBC cells in vitro. We did these experiments in four cell lines that have previously been demonstrated to express AR: MDA-MB-453, ACC-422, SUM-185, and MDA-MB-231 cells. Notably, the MDA-MB-453 and ACC-422 cells have high expression of AR (including when compared to ER+ cell lines), with SUM-185 cells demonstrating intermediate levels of AR expression, and MDA-MB-231 cells with low AR expression[10]. Clonogenic survival assays were performed in MDA-MB-453 cells. A one-hour pretreatment with apalutamide was sufficient to radiosensitize MDA-MB-453 cells (Fig. 1a, radiation enhancement ratios [rER]: 1.34-1.41) and ACC-422 cells[20]. Treatment with darolutamide, a structurally unique AR antagonist, did not affect radiosensitivity of MDA-MB-453 (Fig. 1b, rER: 1.03-1.11), SUM-185 (Fig. 1c, 0.96-1.03), or ACC-422 cells (Fig. 1d, 1.04–1.11). TNBC cells with low AR expression (MDA-MB-231) were not radiosensitized by apalutamide (Fig. 1e, rER: 0.96-1.02) or darolutamide (Fig. 1f, rER: 1.00-1.03). These findings suggest differences in the ability of AR antagonists to sensitize AR+ TNBC cells to RT in vitro. Interestingly, darolutamide has been shown to be more effective than apalutamide or enzalutamide at inhibiting AR-mediated transactivation[21]. The bioavailability of darolutamide, however, is much lower than that of apalutamide or enzalutamide, which may have an effect on the radiosensitization conferred via darolutamide inhibition[22].

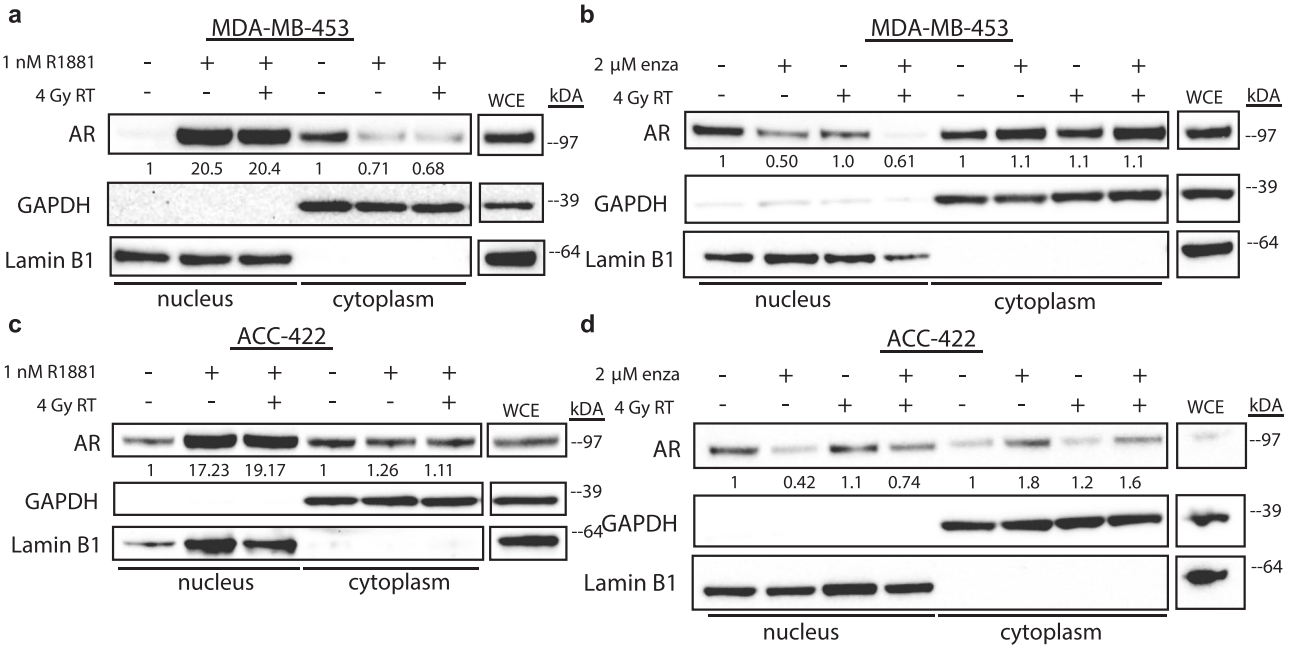

Fig. 2 | Fractionation of AR expression following stimulation or inhibition with RT. Nuclear fractionation experiments were performed in (**a**) MDA-MB-453 and (**c**) ACC-422 cells initially cultured in CSS, then treated with R1881, RT, or R1881+RT. R1881 was given one hour prior to RT, and cells were harvested one hour after RT. Experiments were also performed in (**b**) MDA-MB-453 and (**d**) ACC-422 cells cultured in FBS, treated with enzalutamide (enza), RT, or enzalutamide + RT. Enzalutamide was given one hour prior to RT, and cells were harvested one hour after RT. Experiments were performed in triplicate, and quantifications represent the average AR protein expression relative to GAPDH or Lamin B1 expression, respectively. Relative expression of AR in treated conditions was then determined relative to the expression of AR in the nuclear or cytosolic fraction of cells without R1881/RT (**a**, **c**) or enza/RT (**b**, **d**) treatment. AR: androgen receptor, RT: radiation therapy, CSS: charcoal-stripped serum.

Nuclear localization of AR is blocked with pharmacologic AR inhibitors, but AR continues to localize to the nucleus following radiation treatment

Next, we sought to understand the mechanism of AR-inhibitor mediated radiosensitization in AR+ TNBC models and hypothesized that AR may be acting as a canonical transcription factor to mediate gene expression changes after radiation by nuclear translocation and promoter or enhancer region binding with transcriptional activation. First, we confirmed that pharmacologic AR inhibitors were effectively blocking AR nuclear translocation in AR+ TNBC models by assessing the cellular localization of AR using nuclear and cytosolic fractionation. To do this, MDA-MB-453 and ACC-422 cells were cultured in hormone-deplete conditions for 48 hours and stimulated with the androgen (R1881) for one hour before cell harvesting. When stimulated for one hour with 1 nM R1881, AR translocates to the nucleus, and this is partially blocked with the addition of 2 μM enzalutamide (1 hour pretreatment before R1881 stimulation) in MDA-MB-453 (16% reduction, Supplementary Fig. 1a) and ACC-422 (24% reduction, Supplementary Fig. 1b) cells. In cells treated with FBS, which contains ligand activating-hormones, including androgens, AR is located in the nuclear fraction. Treatment for two hours with the second-generation anti-androgens apalutamide, darolutamide, or enzalutamide blocks AR nuclear translocation in both cell lines (24-66%, Supplementary Fig. 1a, b). Interestingly, apalutamide and enzalutamide more efficiently blocked AR nuclear translocation in MDA-MB-453 cells compared to darolutamide, suggesting that the structural differences in these inhibitors[23] may affect their ability to block AR in some contexts in breast cancer models. These findings together suggest that pharmacologic inhibitors of AR are effective at blocking AR nuclear translocation, resulting in some increased accumulation of AR in the cytoplasm in AR+ TNBC models in vitro and thus may be able to differentially regulate transcriptional activity.

To further determine how radiation was affecting cellular localization of AR in the presence or absence of AR inhibition, cellular fractionation experiments were performed on AR+ TNBC cell lines treated with radiation in the context of AR stimulation or inhibition. First, cells were cultured in hormone-deplete conditions for 48 hours, then stimulated with R1881 for one hour before 4 Gy RT and harvested one hour after radiation. As expected, treatment with the AR-agonist R1881 induced AR nuclear translocation, and this was sustained with radiation treatment in both MDA-MB-453 and ACC-422 cells (Fig. 2a, c). In cells treated with media containing FBS, AR was again observed in the nucleus under baseline conditions; however, AR inhibition with enzalutamide was sufficient to block AR nuclear translocation (50-58% reduction, Fig. 2b, d). Notably, AR remained in the nucleus following RT, but AR accumulated in the cytoplasm when enzalutamide was given one hour prior to RT in MDA-MB-453 and ACC-422 cells (10-60% increase in cytoplasmic AR relative to NT, Fig. 2b, d). These findings suggest that AR is indeed present in the nucleus immediately following radiation treatment; however, treatment with enzalutamide is sufficient to block AR nuclear translocation and may inhibit AR's activity in its canonical role of a transcription factor. Therefore, as it has been previously reported that treatment with enzalutamide before radiation provides increased radiosensitization[9–11], we sought to understand how AR may be promoting DNA repair and resistance to RT in AR+ TNBC models.

Transcriptomic analyses in AR+ TNBC cell lines treated with R1881 or RT alone

A canonical role for AR is to function as a transcription factor and regulate expression of target genes in response to hormone signaling. To understand how AR may be controlling transcriptional regulation in response to ionizing radiation, we performed bulk RNA-sequencing on AR+ ACC-422 and MDA-MB-453 cells. These cells were first cultured in hormone deplete conditions, treated with 1 nM R1881 or 4 Gy RT, and harvested 24 hours after treatment (Fig. 3a). Sequencing was also performed on cells treated with the combination of R1881 with RT where R1881 treatment was administered 24 hours prior to RT, and cells were harvested 24 hours after RT (Fig. 3a). Treatment with R1881 alone resulted in numerous differentially expressed genes in both ACC-422 (668 genes, Fig. 3b) and

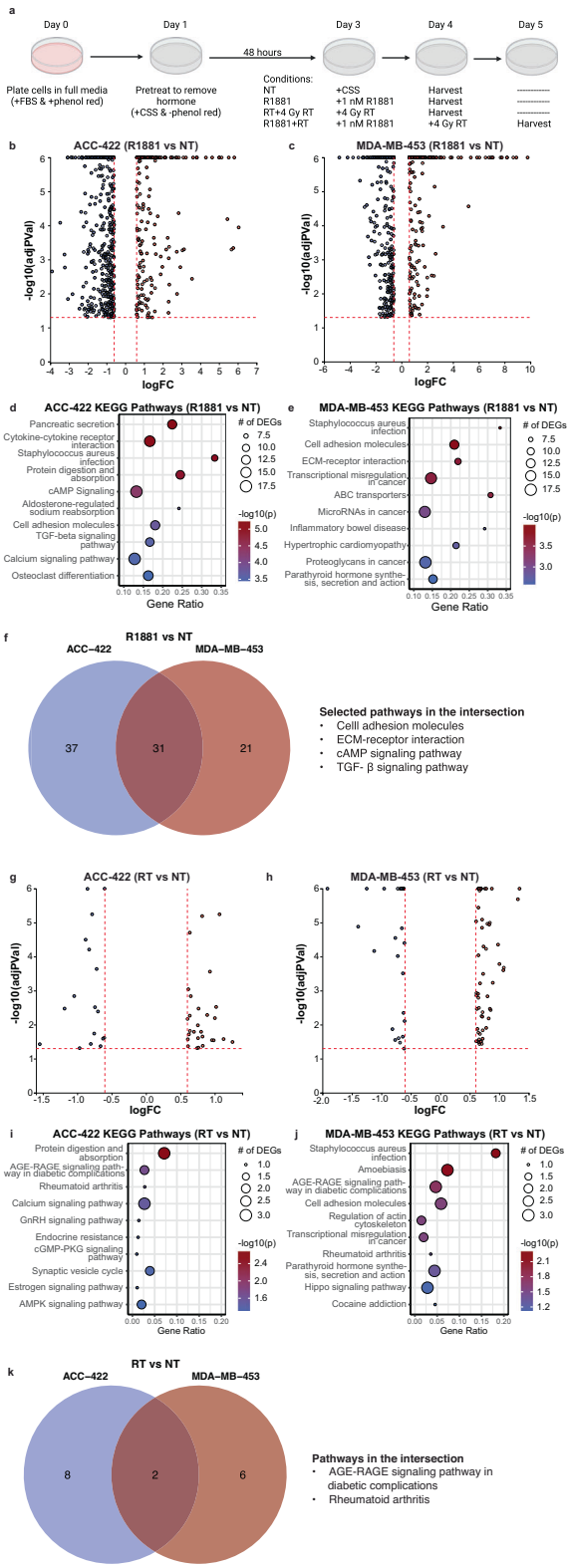

Fig. 3 | Analysis of differentially expressed genes and pathway changes in AR+ TNBC models after single treatments. a Schematic of treatment for RNA-seq samples in all treatment groups, including the no-treatment control (NT), radiation therapy (RT) only, synthetic androgen (R1881) only, and the combination of RT and R1881. ACC-422 and MDA-MB-453 cells were pretreated in charcoal-stripped serum (CSS) for 48 hours prior to stimulation with R1881 (24 hours), treatment with 4 Gy RT, or combination treatment (24-hour pretreatment with R1881 before RT). All cells were harvested 24 hours post-treatment. Volcano plots of differentially expressed genes (DEGs) in (**b**) ACC-422 or (**c**) MDA-MB-453 cells treated with R1881 compared to NT cells, with upregulated genes in red and downregulated genes in blue. The red dashed lines represent the thresholds defining the genes used in the pathway analysis: adjusted p-value threshold 0.05 and log fold change (logFC) threshold 0.6. Pathway analysis identifies pathways that are significantly affected by treatment of R1881 compared to untreated cells in (**d**) ACC-422 and (**e**) MDA-MB-453 cells, where the x axis is the ratio of significantly differentially expressed genes in a pathway to the total number of genes in a pathway. **f** Venn diagram comparing significant pathways in each cell line treated with R1881 and selected pathways listed in which androgen receptor (AR) has previously been shown to play a role. Volcano plots also show differentially expressed genes in (**g**) ACC-422 or (**h**) MDA-MB-453 cells treated with RT compared to untreated cells. Changed pathways for cells treated with RT compared to untreated cells were also assessed in (**i**) ACC-422 and (**j**) MDA-MB-453 cells. **k** Venn diagram comparing significant pathways in each cell line treated with RT, with pathways significant in both cell lines listed. Panel (**a**) was created with BioRender and (**b**), (**c**), (**g**), and (**h**) were created with iPathwayGuide (AdvaitaBio)[31]. TNBC: triple-negative breast cancer.

MDA-MB-453 (701 genes, Fig. 3c) cells compared to control. When pathway analysis was performed on the differentially expressed gene lists, multiple pathways were found to be enriched in each cell line (ACC-422: 68 pathways, Supplementary Table 1; MDA-MB-453: 52 pathways, Supplementary Table 2). Of these pathways, 31 were enriched in both cell lines when treated with R1881, including Cell Adhesion Molecules, ECM-receptor Interaction, cAMP Signaling Pathway, and TGF-β signaling, with androgens having a previously reported role in each pathway[24–26] (Fig. 3d, e, f). On the other hand, treatment with RT alone resulted in far fewer differentially expressed genes relative to control in both cell lines at this early time point (Fig. 3g, ACC-422: 45 genes; Fig. 4h, MDA-MB-453: 88 genes). Concordantly, pathway analysis of these smaller differentially expressed gene lists yielded fewer enriched pathways in each cell line, with 10 and 8 pathways enriched in ACC-422 and MDA-MB-453 cells, respectively (Supplementary Tables 3, 4). Of these pathways, the cell lines share AGE-RAGE Signaling Pathway in Diabetic Complications and Rheumatoid Arthritis (Fig. 3i, j, k). This is consistent with previous reports that androgen depletion and ionizing radiation may have pathogenic roles in both diabetes and rheumatoid arthritis[27–30].

Transcriptomic Analyses in AR+ TNBC cell lines treated with R1881+RT

Next, to determine contextual differences in gene expression with the combined treatment of AR activation and RT, we conducted differential gene expression analysis on cells treated with RT in combination with R1881 relative to cells receiving no treatment (NT). These analyses identified 1,008 differentially expressed genes in ACC-422 cells (Figs. 4a), and 1,077 differentially expressed genes in MDA-MB-453 cells (Fig. 4b). Pathway analysis was again performed on these gene lists to identify pathways that are overrepresented with combination treatment, yielding 70 enriched pathways in ACC-422 cells and 66 enriched pathways in MDA-MB-453, with 37 of these pathways overlapping between the cell lines (Fig. 4c, d, e; Supplementary Table 5,6). There was significant pathway overlap identified between cells treated with R1881+RT and those treated with R1881 alone. Notably, 45 of the 68 identified pathways with R1881 treatment alone were also overrepresented with combination treatment of R1881+RT in ACC-422 cells. Similarly, 37 of the 52 identified pathways following R1881 treatment were also overrepresented with combination treatment in MDA-MB-453 cells. Furthermore, 22 of the pathways occurred in both R1881 vs. NT and R1881+RT vs. NT were identified in both cell lines (Fig. 4f).

To identify changes that are due to R1881 treatment in the context of RT, we compared cells treated with RT alone to cells treated with R1881+RT. In this comparison, there were 1,006 differentially expressed genes in ACC-422 cells (Figs. 4g) and 1,141 differentially expressed genes in MDA-MB-453 cells (Fig. 4h). Pathway analysis was performed in both cell

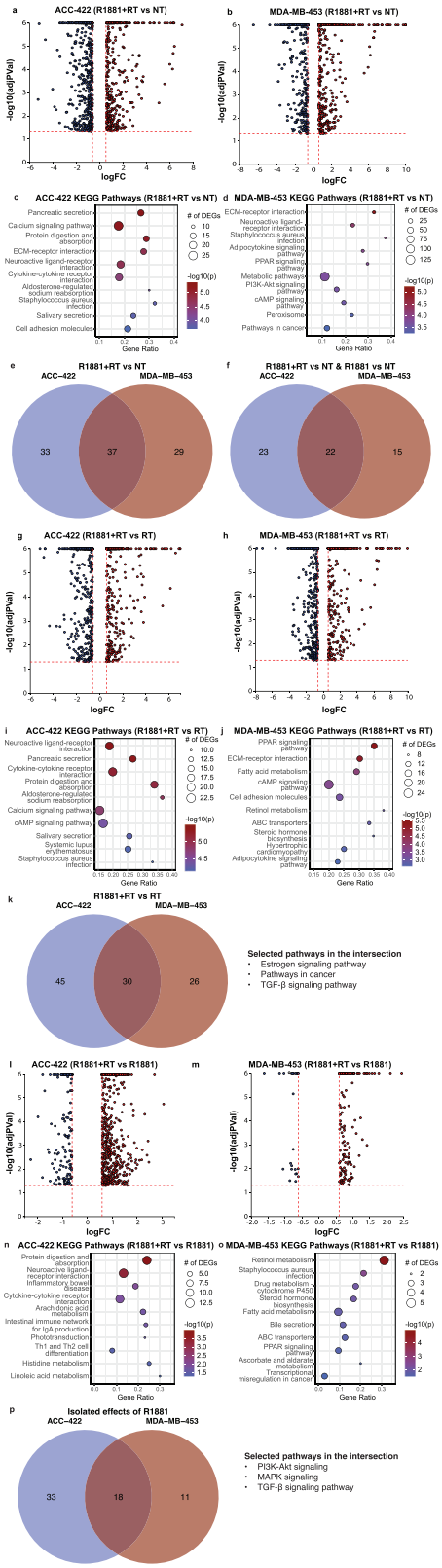

Fig. 4 | Analysis of differentially expressed genes and pathway changes in ACC-422 and MDA-MB-453 cells for combination treatments. Volcano plots of differentially expressed genes (DEGs) in (**a**) ACC-422 or (**b**) MDA-MB-453 cells treated with R1881+RT compared to untreated (NT) cells. Pathway analysis identifies pathways that are significantly affected by treatment of R1881+RT compared to untreated cells in (**c**) ACC-422 and (**d**) MDA-MB-453 cells. **e** Venn diagram comparing significant pathways in each cell line treated with R1881+RT. **f** Venn diagram comparing significant pathways in each cell line that occur in each cell line in both the R1881+RT vs NT condition and the R1881 vs NT condition. Volcano plots also show differentially expressed genes in (**g**) ACC-422 or (**h**) MDA-MB-453 cells treated with R1881+RT compared to cells treated with RT alone. Changed pathways for cells treated with R1881+RT compared to cells treated with RT alone were also assessed in (**i**) ACC-422 and (**j**) MDA-MB-453 cells. **k** Venn diagram comparing significant pathways in each cell line treated with R1881+RT vs RT and a list highlighting selected pathways in the intersection. Similarly, volcano plots also show differentially expressed genes in (**l**) ACC-422 or (**m**) MDA-MB-453 cells treated with R1881+RT compared to cells treated with R1881 alone. Affected pathways for cells treated with R1881+RT compared to cells treated with R1881 alone were also assessed in (**n**) ACC-422 and (**o**) MDA-MB-453 cells. **p** Venn diagram comparing significant pathways in each cell line looking at the isolated impact of R1881 stimulation (pathways occurring in both the R1881+RT vs RT condition and the R1881 vs NT condition) with selected pathways which are likely to contribute to cell growth, and thus may present targets, highlighted from the intersection. **a**, **b**, **g**, **h**, **l**, **m** were created with iPathwayGuide (AdvaitaBio)[31]. RT radiation therapy.

lines (Fig. 4i, j), and complete lists of significant pathways are recorded in Supplementary Table 7 (ACC-422) and Supplementary Table 8 (MDA-MB-453). These analyses identified 75 pathways to be overrepresented in ACC-422 cells and 56 in MDA-MB-453 cells, with 30 of these pathways observed in both pathways (Fig. 4k). Additionally, of the 75 pathways in ACC-422 (R1881+RT vs. RT), 51 were also identified with R1881 treatment alone (R1881 vs. NT). These pathways include the Estrogen Signaling Pathway, Pathways in Cancer, and the TGF-β Signaling Pathway, among others. These same pathways were also among the pathways identified in MDA-MB-453 cells in both the R1881+RT vs. RT and R1881 vs. NT treatment conditions, suggesting that R1881 treatment is modulating changes to these signaling pathways in the context of RT.

To identify specific changes that are due to radiation in the context of R1881 treatment, we compared cells treated with R1881 alone against combination treated cells (R1881+RT vs. R1881). Interestingly, there were only 160 differentially expressed genes in MDA-MB-453 cells (Fig. 4m), corresponding to 15 overrepresented pathways (Fig. 4o; Supplementary Table 9). Despite identifying 812 differentially expressed genes in ACC-422 cells (Fig. 4l; Supplementary Table 10), pathway analysis identified only 10 overrepresented pathways (Fig. 4n), none of which overlapped with those found in the 15 pathways identified in the MDA-MB-453 cell line. These findings are consistent with the relatively lower number of differentially expressed genes and overrepresented pathways with radiation treatment alone (RT vs. NT) compared to treatment with R1881 alone (R1881 vs. NT).

While we identified many pathway differences as a result of treatment with R1881, RT, and combination treatments, we also recognized multiple recurring pathways in treatment conditions involving treatment with R1881 alone or with treatment of R1881 in combination with RT. There were 29 of these pathways in the MDA-MB-453 cell line and 51 in the ACC-422 cell line, with 18 of these pathways identified in both cell lines (Fig. 4p). These common pathways included the PI3K-Akt signaling pathway, the MAPK signaling pathway, and the TGF-β signaling pathway. These pathways play important roles within the cell, specifically regulating cell growth and proliferation, and therefore may be important in contributing to cellular growth following treatment with R1881 alone or in combination with RT. Looking more specifically at MAPK pathway genes in the MDA-MB-453 cell line across all treatment conditions, we see that all differentially expressed genes recorded respond in the same direction in all comparisons measuring R1881 stimulation (R1881 vs. NT, R1881+RT vs. NT, R1881+RT vs. RT; Fig. 5). We saw a similar trend in the ACC-422 cell line (Supplementary Fig. 2). Many of the differentially expressed genes in this KEGG pathway are specifically involved in Raf-MEK-ERK signaling (including *PRAAK2, EGFR, ERBB2, MAP3K5, MAPK11, MEF2C, MAP3K20, MAPK10*). We also found differential protein abundance of MAPK-related proteins using reverse-phase protein array (RPPA) in hormone-replete conditions

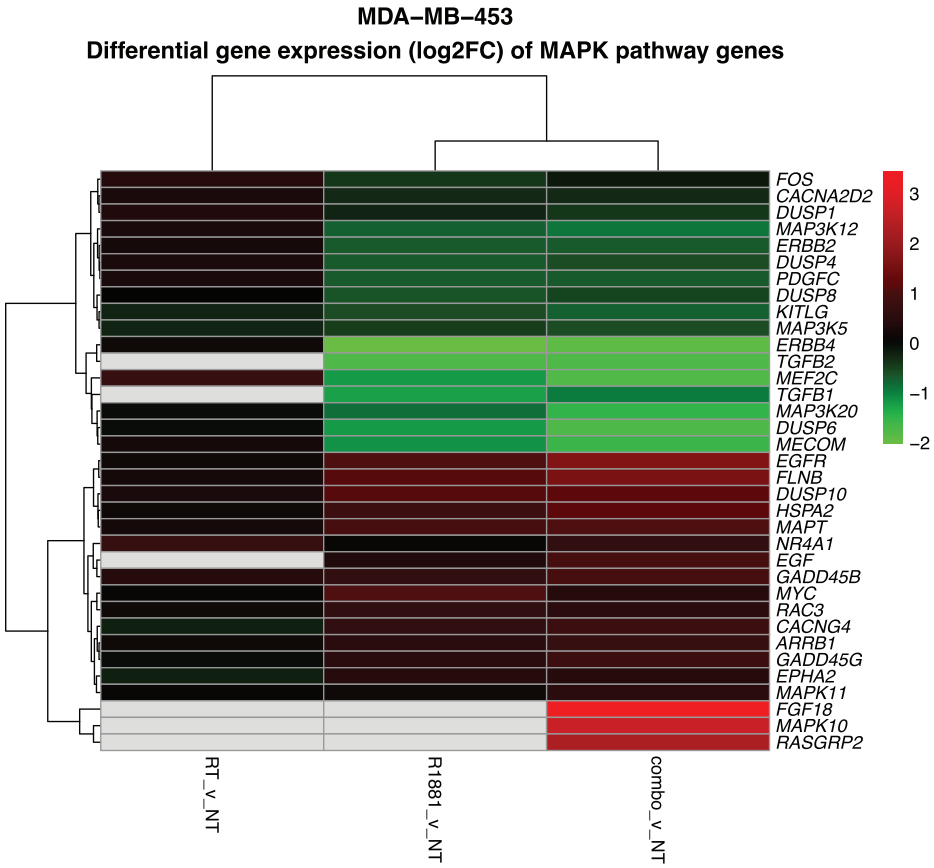

Fig. 5 | Gene expression changes in the MAPK pathway in MDA-MB-453 cells under various treatment conditions. A heat map displaying differentially expressed genes from within the MAPK KEGG pathway in MDA-MB-453 cells for each treatment condition along the x-axis, with log2 fold change (log2FC) indicated by the color scale on the heatmap and differentially expressed genes along the y-axis. Red indicates higher gene expression in the first condition relative to the second in the comparison, and green indicates lower expression in the first condition relative to the second. Grey boxes indicate genes with no reported log2FC value for that comparison, resulting from genes with <1 read per sample on average for the compared treatments being removed from the analysis. RT: radiation therapy; NT: no treatment; combo: RT and R1881.

(Supplementary Fig. 3). Taken together, these data suggest that MAPK signaling may be an important intermediary for androgen-signaling in AR+ TNBC models.

ERK overexpression reduces AR-inhibitor mediated radiosensitization

Hypothesizing that the MAPK/ERK pathway acts as an intermediary between AR transcription factor function and radioresistance, we aimed to assess if stimulating MAPK/ERK signaling reduces the effect of AR inhibition in response to radiation. To test this, we overexpressed constitutively active ERK2 in ACC-422 cells. On day three after transfection, the ACC-422 cells were pretreated for 1 hour with apalutamide and irradiated and assessed for clonogenic survival (Fig. 6a). The sham transfected cells were radiosensitized by 5μM apalutamide with an enhancement ratio of 1.22 whereas the ERK overexpressing cells were not radiosensitized by apalutamide with an enhancement ratio of 0.96 (Fig. 6b, c). This suggests that the MAPK/ERK pathway mediates a component of AR-driven radioresistance (Fig. 7).

Discussion

Previous work has demonstrated that AR is a mediator of radioresistance both in AR+ TNBC[9–11] and prostate cancer models[16–18]. Our work has demonstrated that AR inhibition or knockdown radiosensitizes AR+ TNBC cells[9,10]; however, there are differences in the abilities of AR inhibitors to radiosensitize AR+ TNBC[20] (Fig. 1). These observed differences may be due, at least in part, to variation in the bioavailability of the AR inhibitors. Under baseline conditions, AR is located both in the cytoplasm and in the nucleus of the cell but is responsive to stimulation with R1881, a synthetic androgen, or AR inhibition with the second-generation anti-androgens, apalutamide, darolutamide, and enzalutamide (Supplementary Fig. 1). While this previously has been explored in prostate cancer models, these findings confirm a canonical role for AR as a nuclear hormone transcription factor that is responsive to both stimulation and inhibition in our AR+ TNBC models. In addition, our data suggest that AR is present in the nucleus following RT (Fig. 2), and AR may be, at least in part, driving a transcriptional program in response to stimulation and RT (Figs. 3 and 4). Further, our data suggest a role for AR in the regulation of MAPK/ERK signaling following RT (Figs. 4–6, Supplementary Figs. 2 and 3), indicating that AR may be regulating changes at the transcriptional level resulting in the observed AR-mediated radioresistance by promoting DNA repair as previously observed following treatment with AR inhibition in AR+ TNBC models[9,10]. These findings expand on non-genomic roles for AR in the radiation response that have previously been addressed in AR+ breast and prostate cancer models[9,10,17,18]. Further, our findings are in line with previous findings in prostate cancer, where inhibition of MEK is sufficient to modulate the radiation response in AR+ prostate models[32]. Interestingly, in prostate cancer, MAPK/ERK signaling has also been shown to influence AR expression levels and therefore modulate downstream AR targets, suggesting there may be additional feedback loops at play between AR and MAPK/ERK signaling[32,33].

Notably, in both AR+ TNBC cell lines tested, there are far more differentially expressed genes between cells treated with R1881 alone compared to control and those treated with RT alone compared to control. This suggests that androgen signaling is important for the regulation of gene expression in AR+ TNBC models and is perhaps not surprising. While non-canonical roles for AR have recently been described[34–36], AR canonically functions as a transcription factor that is activated immediately after ligand binding. Thus, at the early time points selected for this study, the ligand bound AR can dimerize and translocate to the nucleus to activate transcription, with early response genes being induced within four hours of stimulation[37,38]. Conversely, radiation effects are delayed and can take days for changes to be noted[39,40]. Thus, this study evaluates relatively early effects of AR stimulation and RT on

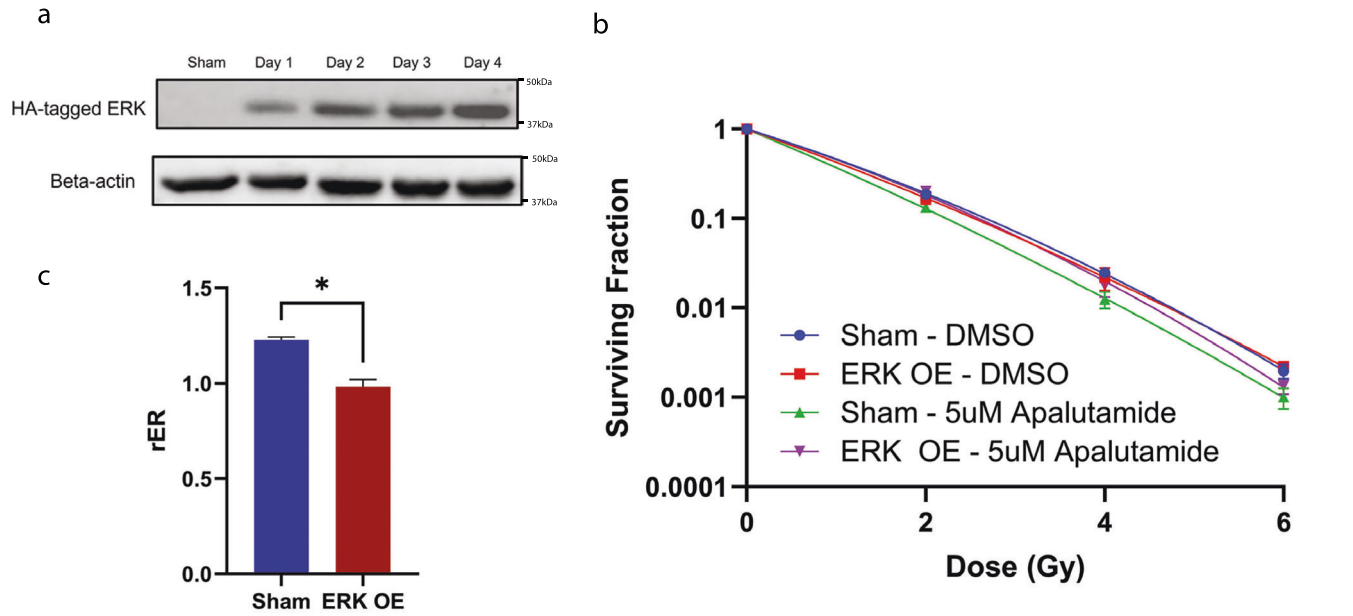

Fig. 6 | ERK overexpression blunts the radiosensitizing effect of apalutamide. Constitutively active ERK was overexpressed (OE) in ACC-422 cells and then assessed for radiosensitization with apalutamide. **a** Western blot demonstrating overexpression of HA-tagged constitutively active ERK. Clonogenic survival assay curves (**b**) and radiation enhancement ratios (rER) with 5 μM apalutamide (**c**) of both sham transfected and ERK-overexpressing ACC-422 cells. Experiments were performed in triplicate and graphed as mean ± SEM. * $p < 0.05$. SEM: Standard error of the mean.

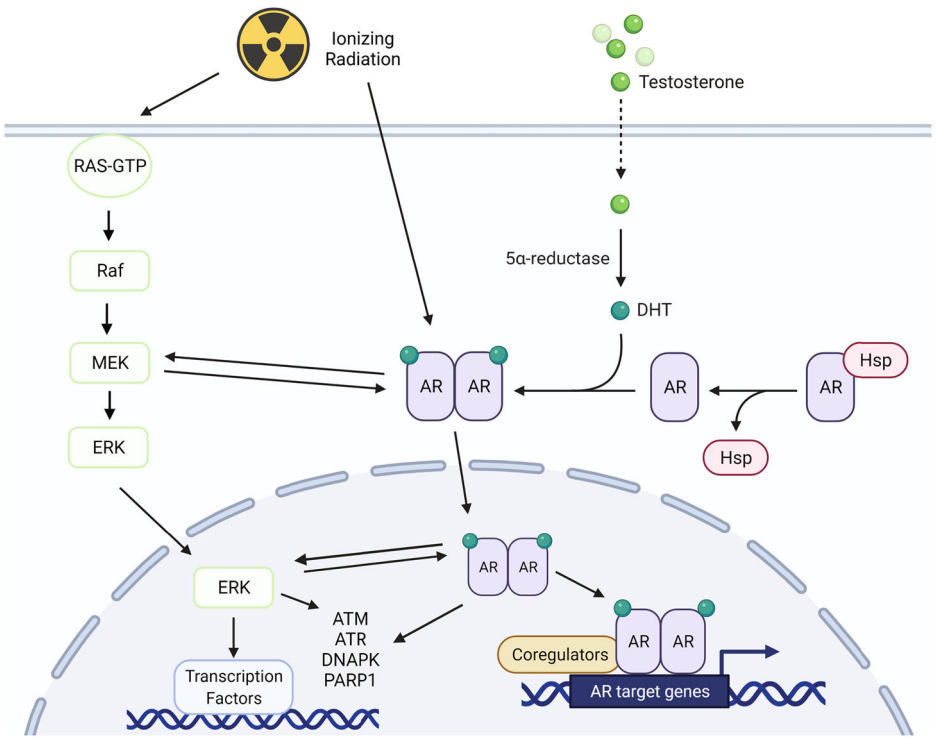

Fig. 7 | Proposed mechanism for AR and MAPK signaling pathway interplay in radioresistance. Androgen receptor (AR) and MAPK signaling pathways are activated following radiation therapy (RT), and interplay between pathways may be promoting radioresistance in AR+ triple-negative breast cancer (TNBC) models and mediating DNA repair following RT.

AR activity, and future studies will look at later time points to determine how RT influences AR's canonical transcriptional role. Additionally, while our analyses do not specifically compare AR signaling in prostate and breast cancer models directly as others have[6], our findings agree with previous reports and hypotheses that AR is contributing, at least in part, to tumor growth in AR+ TNBC models.

Previous work by our group and others has demonstrated that inhibiting AR results in decreased phosphorylation of DNAPKcs[9,18,41], leading to a delay in dsDNA break repair with AR inhibitors following RT in breast and prostate models. Here we highlight the role for the MAPK cascade in response to ionizing radiation (Fig. 7) which has previously been noted in other cancers including glioma, non-small cell lung cancer, and fusion-negative rhabdomyosarcoma[42–46]. In a melanoma cohort, AR inhibition improved response to BRAF/MEK, and AR signaling may promote resistance to BRAF/MEK-targeted therapy[47]. These findings parallel work done in prostate cancer where activation of AR has been shown to activate the Ras-Raf-1 signaling cascade and ERK phosphorylation[48,49]. In addition, with radiation, targeting of MAPK signaling and specifically inhibition of MEK/ERK results in decreased ERK phosphorylation and increased radiosensitivity[32]. These changes in radiosensitivity are due, at least in part

to a delay in dsDNA repair due to impaired efficiency of NHEJ and HR[43,44]. This represents a non-canonical role for AR in mediating NHEJ activity through phosphorylation of DNAPK. Therefore, taken with our findings, our working model indicates that the use of AR inhibitors including enzalutamide may reduce MAPK signaling resulting in aberrations to DNA repair pathways. Future studies, however, are needed to identify the specific role for AR and MAPK related transcripts in this process.

There are additional limitations of our study that should also be considered. First, here we used cell line models that can be cultured in the presence or absence of media containing hormones. In our study, we have used multiple culture conditions to try to provide a more complete understanding of the effects of AR inhibitors when used in combination with RT. Our studies, however, were performed using cell culture models and have not been expanded into 3D culture systems using mammospheres or in vivo animal models. While these studies are globally mechanistic in nature, future studies will continue to validate this work in increasingly diverse model systems. While we show that MAPK/ERK signaling plays a downstream role in AR signaling after radiation via ERK overexpression, our studies do not explore ERK inhibition or confirm the nature and magnitude of the AR and MAPK/ERK signaling interaction. The RNA-seq data presented here indicate that canonical AR transcription factor functions play a role in modulating MAPK/ERK signaling pathway gene expression. However, in other contexts AR has been shown to impact MAPK/ERK signaling through non-genomic mechanisms, so future studies will aim to understand the mechanism underlying the effect of AR on MAPK/ERK signaling in the context of radiation[50,51].

Future studies will also consider the possibility that our model may lack intermediary steps that could be involved in the AR-inhibitor mediated radiosensitization phenotype. One example could include the minor spliceosome. While we demonstrate that AR may play a role in regulating MAPK signaling, transcripts in the MAPK signaling pathway are highly regulated by minor spliceosome activity[52], and knockdown of the minor spliceosome results in the inhibition of DNA repair[53]. Therefore, our model may also rely on splicing for radiosensitization with AR inhibition. These studies were also performed in vitro using models that do not account for the role of the immune system or tumor microenvironment[54]. In prostate cancer models, AR has been demonstrated to repress IFNγ expression resulting in immunotherapy resistance[55]. Future and ongoing studies will investigate these limitations by using immunocompetent in vivo models. Additionally, there are other enriched pathways (i.e., PI3K-AKT and TGF-β) that future studies will aim to study in the context of AR-mediated radiosensitization in AR+ breast cancer.

Our findings contribute to a larger body of literature demonstrating that the use of AR inhibitors alone or in combination with radiotherapy may be an important addition to the treatment armamentarium for AR+ TNBC. Results from clinical trials demonstrate that AR inhibitors, specifically enzalutamide, are well tolerated and have response rates of ~30%[1]. Ongoing work is needed to understand the mechanisms by which AR is contributing to tumorigenesis in AR+ breast cancer models. Most notably, there is a critical need for biomarkers of response that can be used to effectively identify patient populations that will benefit from treatment with AR inhibitors. While AR has been identified as a biomarker of radioresistance when expressed in AR+ TNBC, additional work has demonstrated that it may play a different role in the context of AR+/ER+ breast cancers[12,14]. Therefore, future studies are needed to identify other biomarkers that can impact radiosensitivity in a variety of contexts to inform appropriate clinical strategies for women with AR+ breast tumors.

Methods

Cell culture

Cells were grown in an incubator at 37°C with 5% CO_2. MDA-MB-453 cells were obtained from ATCC (RRID:CVCL_0418) and grown in DMEM media (ThermoFisher 11965092) containing 1% penicillin/streptomycin (pen/strep; ThermoFisher 15070063) and 10% Fetal Bovine Serum (FBS; Atlanta Biologicals S11550H). ACC-422 cells (RRID:CVCL_1408) were grown in MEM media (ThermoFisher 11095080) containing 1X Insulin-Transferrin-Selenium-Ethanolamine (ITS-X; Gibco 51500056), 1% pen/strep, and 15% FBS. Cell lines were authenticated by DNA fingerprinting using short tandem repeat (STR) profiling. Cells were routinely tested for mycoplasma using the MycoAlert Mycoplasma Detection kit (Lonza LT07).

Clonogenic survival assay

Cells were plated as a single-cell suspension in six-well plates in FBS media and left to adhere overnight. Drug-containing media was added 1 hour before radiation. After 1-2 weeks, cells were fixed with methanol/acetic acid and stained with crystal violet. Colonies were counted and the surviving fraction was fit using a linear quadratic method.

Western blotting

Cells were seeded in 10 cm dishes and allowed to adhere overnight before being stripped of hormones using phenol-red free media. For ACC-422 cells, MEM media (#51200-028) was supplemented with 15% charcoal stripped serum (CSS, Atlanta Biologicals #S11650H), 1% pen/strep, 2 mM L-glutamine (Sigma G7313) and 1X ITS-X. For MDA-MB-453 cells, DMEM media (#21063-029) was supplemented with 10% CSS, 1% pen/strep. Cells were cultured in hormone deplete conditions for 48 hours before stimulation with 1 nM R1881 and harvested after 1 hour of stimulation. For experiments with cells cultured in FBS, drug treatments were administered 1 hour before harvesting cells. For experiments with radiation treatment, cells were treated with a pharmacologic agent, where denoted, 1 hour before 4 Gy RT, and harvested 1 hour after radiation. To harvest cells, they were washed twice with cold PBS and harvested by scraping. Nuclear and cytoplasmic cellular fractionations were subsequently separated using NE-PER Nuclear and Cytoplasmic Extraction Reagents (Thermo Scientific 78835). Lysates were standardized using the Pierce BCA Protein Assay Kit (Thermo Scientific 23227) and RIPA buffer (Thermo Scientific 89901) containing phosphatase and protease inhibitors (Sigma #PHOSS-RO, #CO-RO). Following standardization, samples were sonicated, reduced with 4x NU-PAGE buffer (Life Technologies NP0007) and 2% β-mercaptoethanol. For nuclear fractionation experiments, reduced lysates were run on gels and probed for AR (1:1000; Millipore PG-21 #06-680, RRID:AB_310214), LaminB1 (1:1000; CST 12586, RRID:AB_2650517), and GAPDH (1:1000; CST 2118L, RRID:AB_561053). The expression of exogenous ERK was validated by probing for the HA-tag (1:1000; CST 3724S, RRID:AB_1549585 and beta-actin (1:1000; CST 3700S, RRID:AB_2242334). An anti-rabbit secondary was used (1:10,000; CST 7074S, RRID:AB_2099233). Quantification of western blots was performed using ImageJ software.

RNA-sequencing

MDA-MB-453 and ACC-422 cells were plated in media containing FBS and left to adhere overnight. The following day, cells were pretreated in media without phenol red containing CSS instead of FBS for 48 hours. After this pretreatment, cells were stimulated with 1 nM R1881, 2 μM enzalutamide, or 4 Gy RT for 24 hours. Cells treated with a combination of R1881 with RT or enzalutamide with RT first received a 24-hour pretreatment with R1881, followed by 4 Gy RT, and RNA was collected 24 hours post-RT (Fig. 3A). For each sample, RNA was collected using TRIzol and isolated using the miRNeasy mini kit (Qiagen 217004). Poly(A) mRNA library preparation and RNA sequencing was performed by the Advanced Genomics Core at the University of Michigan using Illumina sequencing on the NovaSeq flow cell platform. Three replicates of the samples were submitted for each condition. Schematic of treatment outline is shown in Fig. 3A.

Transcriptomic analysis

Raw read counts obtained from the Advanced Genomics Core at the University of Michigan were aligned against genome version hg38 using HISAT2 (v2.1.0)[56]. Aligned reads were mapped to genes from GRCh38.84 Ensembl annotation[57] using htseq-count (v2.0.3)[58]. These count matrices were analyzed for differential gene expression analysis with DeSeq2

(v1.36.0)[59]. The Benjamini-Hotchberg method was applied to adjust for multiple testing correction with a significance threshold $p < 0.05$ for differentially expressed genes. All genes, their log2 fold change value, and their adjusted p-values were submitted for analysis via iPathwayGuide (AdvaitaBio; v17.0)[31]. iPathwayGuide uses two metrics to nominate significant pathways: (1) over-representation analysis, which looks at the ratio of differentially expressed genes in a pathway to the total number of genes in that pathway, and (2) total perturbation accumulation, which combines fold change and "total accumulation", which measures the propagation of the effect of the expression of upstream genes on downstream genes based on documented gene interactions. A pathway is determined to be significant if the combined p-values from the two analyses is significant. The p-value, total perturbation accumulation p-value (pAcc), over-representation analysis p-value (pORA), and the combined pACC and pORA (pComb) included in all tables were calculated with iPathwayGuide (AdvaitaBio)[31]. NA indicates pAcc (and therefore pComb) were not calculated by iPathwayGuide.

Reverse-phase protein array (RPPA)

Cells were seeded in 6-well plates before treatment with 1 μM enzalutamide (MDV3100; MedChem Express HY-70002) or vehicle control (DMSO). Drug treatment was administered 24 hours prior to radiation treatment (4 Gy). Following radiation, cells were harvested at the indicated time points using cell scrapers. Cells were lysed with RIPA buffer supplemented with cOmplete Mini protease (PHOSS-RO) and phosSTOP (COEDTAF-RO). Bond-Breaker TCEP solution (Pierce Biotechnology) was added at 1/10th volume and samples were boiled at 95 °C and stored at -80 °C prior to analysis. A schematic of treatment is outlined in Supplementary Fig. 3A.

After protein lysates were prepared as described above, the lysates were serially diluted (1:2, 1:4, 1:8, and 1:16). An Aushon 2470 arrayer (Quanterix) was used to create a spot array containing all samples for each antibody measured (>100 antibodies in total) on Oncyte Avid nitrocellulose- coated slides (Grace Bio-Labs) according to the manufacturer's instructions. Slides were stored at -80˚C until immunostaining using an automated slide stainer (Dako Link 48), Dako). All antibodies were validated at MD Anderson as well as the Royal College of Surgeons, Dublin, Ireland. Scanned slides were analyzed using MicroVigene software V.5.1 (VigeneTech). Spot intensities were generated using MicroVigene software where a four-parameter logistic-log model, 'SuperCurve' algorithm, was used to fit a curve to each sample[60]. Global sample median normalization was used to normalize all samples with one antibody. Differential expression was measured by comparing treated (Enza, RT, or combination) samples at each time point to the untreated cells within each cell line.

Exogenous ERK expression

ACC422 cells were transfected using lipofectamine 3000 (ThermoFisher L3000015) with a plasmid expressing HA tagged human ERK2 R67SD321N from a blasticidin resistance retroviral vector (Addgene: 53174)[61].

Drugs

Androgen receptor inhibitors were purchased from MedChemExpress (Apalutamide [ARN-509]: HY-16060, Darolutamide [ODM-201]: HY-16985, Enzalutamide: HY-70002). R1881 was provided by the lab of Arul Chinnaiyan at the University of Michigan.

Irradiation

X-ray irradiation was performed at the University of Michigan Experimental Irradiation Core using a Kimtron IC-225. The dose rate of 2 Gy/min was used in keeping with previous studies[9,10,20,62,63]. For in vitro experiments, a 0.1 mm Cu filter was used.

Data availability

The datasets generated and analyzed during the current study are available in GEO, accession number GSE222992.

Code availability

The code for this study is available on GitHub and can be accessed here: https://github.com/B-McBean/AR_Transcriptomics.

Received: 9 June 2025; Accepted: 9 February 2026;
Published online: 24 February 2026

References

1. Traina, T. A. et al. Enzalutamide for the treatment of androgen receptor-expressing triple-negative breast cancer. *J. Clin. Oncol.* **36**, 884–890 (2018).
2. Michmerhuizen, A. R., Spratt, D. E., Pierce, L. J. & Speers, C. W. ARe we there yet? Understanding androgen receptor signaling in breast cancer. *NPJ Breast Cancer* **6**, 1–19 (2020).
3. Kolyvas, E. A., Caldas, C., Kelly, K. & Ahmad, S. S. Androgen receptor function and targeted therapeutics across breast cancer subtypes. *Breast Cancer Res* 24, (2022).
4. Chia, K. M., O'Brien, M., Brown, M. & Lim, E. Targeting the androgen receptor in breast cancer. *Curr Oncol Rep* 17, (2015).
5. Proverbs-Singh, T., Feldman, J. L., Morris, M. J., Autio, K. A. & Traina, T. A. Targeting the androgen receptor in prostate and breast cancer: several new agents in development. *Endocr. Relat. Cancer* **22**, R87–R106 (2015).
6. Ni, M. et al. Targeting androgen receptor in estrogen receptor-negative breast cancer. *Cancer Cell* **20**, 119–131 (2011).
7. Cochrane, D. R. et al. Role of the androgen receptor in breast cancer and preclinical analysis of enzalutamide. *Breast Cancer Res.* **16**, 1–19 (2014).
8. Barton, V. N. et al. Androgen receptor supports an anchorage-independent, cancer stem cell-like population in triple-negative breast cancer. *Cancer Res.* **77**, 3455–3466 (2017).
9. Speers, C. et al. Androgen receptor as a mediator and biomarker of radioresistance in triple-negative breast cancer. *NPJ Breast Cancer* **3**, 1–10 (2017).
10. Michmerhuizen, A. R. et al. Seviteronel, a Novel CYP17 Lyase Inhibitor and Androgen Receptor Antagonist, Radiosensitizes AR-Positive Triple Negative Breast Cancer Cells. *Front Endocrinol. (Lausanne)* **11**, 1–13 (2020).
11. Yard, B. D. et al. A genetic basis for the variation in the vulnerability of cancer to DNA damage. *Nat. Commun.* **7**, 1–14 (2016).
12. Kensler, K. H. et al. Prognostic and predictive value of androgen receptor expression in postmenopausal women with estrogen receptor-positive breast cancer: Results from the Breast International Group Trial 1-98. *Breast Cancer Res.* **21**, 1–11 (2019).
13. Iacopetta, D., Rechoum, Y. & Fuqua, S. A. W. The Role of Androgen Receptor in Breast Cancer. *Drug Discov Today Dis Mech* 9, (2012).
14. Michmerhuizen, A. R. et al. Abstract 6271: Hormone receptor inhibition as a strategy for radiosensitization of breast cancer. *Cancer Res* **80**, 6271–6271 (2020).
15. Tran, C. et al. Development of a second-generation antiandrogen for treatment of advanced prostate cancer. *Science (1979)* **324**, 787–790 (2009).
16. Kakouratos, C. et al. Apalutamide radio-sensitisation of prostate cancer. *Br. J. Cancer* **125**, 1377–1387 (2021).
17. Polkinghorn, W. R. et al. Androgen receptor signaling regulates DNA repair in prostate cancers. *Cancer Discov.* **3**, 1245–1253 (2013).
18. Goodwin, J. F. et al. A hormone-DNA repair circuit governs the response to genotoxic insult. *Cancer Discov.* **3**, 1254–1271 (2013).
19. Werner, C. K. et al. Expression of the androgen receptor governs radiation resistance in a subset of glioblastomas vulnerable to antiandrogen therapy. *Mol. Cancer Ther.* **19**, 2163–2174 (2020).
20. Michmerhuizen, A. R. et al. Androgen and oestrogen receptor co-expression determines the efficacy of hormone receptor-mediated radiosensitisation in breast cancer. *Br J Cancer* 127, (2022).

21. Moilanen, A. M. et al. Discovery of ODM-201, a new-generation androgen receptor inhibitor targeting resistance mechanisms to androgen signaling-directed prostate cancer therapies. *Sci. Rep.* **5**, 1–11 (2015). *2015 5:1*.
22. Bayer HealthCare Pharmaceuticals. Nubeqa (darolutamide) tablets, for oral use [prescribing information]. (2021).
23. Rajaram, P. et al. Second-Generation Androgen Receptor Antagonists as Hormonal Therapeutics for Three Forms of Prostate Cancer. *Molecules* 25, (2020).
24. Ma, W. L., Jeng, L., Bin, Lai, H. C., Liao, P. Y. & Chang, C. Androgen receptor enhances cell adhesion and decreases cell migration via modulating β1-integrin-AKT signaling in hepatocellular carcinoma cells. *Cancer Lett.* **351**, 64–71 (2014).
25. Luthold, C., Hallal, T., Labbé, D. P. & Bordeleau, F. The Extracellular Matrix Stiffening: A Trigger of Prostate Cancer Progression and Castration Resistance? *Cancers (Basel)* 14, (2022).
26. Kim, J., Jia, L., Stallcup, M. R. & Coetzee, G. A. The role of protein kinase A pathway and cAMP responsive element-binding protein in androgen receptor-mediated transcription at the prostate-specific antigen locus. *J. Mol. Endocrinol.* **34**, 107–118 (2005).
27. Navarro, G., Allard, C., Xu, W. & Mauvais-Jarvis, F. The role of androgens in metabolism, obesity, and diabetes in males and females. *Obes. (Silver Spring)* **23**, 713–719 (2015).
28. Nylander, V. et al. Ionizing Radiation Potentiates High-Fat Diet-Induced Insulin Resistance and Reprograms Skeletal Muscle and Adipose Progenitor Cells. *Diabetes* **65**, 3573–3584 (2016).
29. Cutolo, M. et al. Androgens and estrogens modulate the immune and inflammatory responses in rheumatoid arthritis. *Ann. N. Y Acad. Sci.* **966**, 131–142 (2002).
30. Yahyapour, R. et al. Radiation-induced inflammation and autoimmune diseases. *Mil. Med Res* **5**, 1–8 (2018).
31. Draghici, S. et al. A systems biology approach for pathway level analysis. *Genome Res* **17**, 1537–1545 (2007).
32. Ciccarelli, C. et al. Disruption of MEK/ERK/c-Myc signaling radiosensitizes prostate cancer cells in vitro and in vivo. *J. Cancer Res. Clin. Oncol.* **144**, 1685–1699 (2018).
33. Agoulnik, I. U. et al. Target Gene-Specific Regulation of Androgen Receptor Activity by p42/p44 Mitogen-Activated Protein Kinase. *Mol. Endocrinol.* **22**, 2420–2432 (2008).
34. Chia, K. M. et al. Non-canonical AR activity facilitates endocrine resistance in breast cancer. *Endocr. Relat. Cancer* **26**, 251–264 (2019).
35. Ciupek, A. et al. Androgen receptor promotes tamoxifen agonist activity by activation of EGFR in ERα-positive breast cancer. *Breast Cancer Res Treat.* **154**, 225–237 (2015).
36. Trnski, D. et al. SHH-N non-canonically sustains androgen receptor activity in androgen-independent prostate cancer cells. *Sci. Rep.* **11**, 1–11 (2021).
37. Nelson, P. S. et al. The program of androgen-responsive genes in neoplastic prostate epithelium. *Proc. Natl. Acad. Sci. USA* **99**, 11890–11895 (2002).
38. Jin, H. J., Kim, J. & Yu, J. Androgen receptor genomic regulation. *Transl. Androl. Urol.* **2**, 158–177 (2013).
39. Bravatà, V. et al. Radiation-induced gene expression changes in high and low grade breast cancer cell types. *Int J. Mol. Sci.* **19**, 1–15 (2018).
40. Manning, G., Tichý, A., Sirák, I. & Badie, C. Radiotherapy-associated long-term modification of expression of the inflammatory biomarker genes ARG1, BCL2L1, and MYC. *Front Immunol.* **8**, 248356 (2017).
41. Goodwin, J. F. et al. DNA-PKcs-Mediated Transcriptional Regulation Drives Prostate Cancer Progression and Metastasis. *Cancer Cell* **28**, 97–113 (2015).
42. Munshi, A. & Ramesh, R. Mitogen-activated protein kinases and their role in radiation response. *Genes Cancer* **4**, 401–408 (2013).
43. Golding, S. E. et al. Extracellular signal-related kinase positively regulates ataxia telangiectasia mutated, homologous recombination repair, and the DNA damage response. *Cancer Res* **67**, 1046–1053 (2007).
44. Golding, S. E. et al. Pro-survival AKT and ERK signaling from EGFR and mutant EGFRvIII enhances DNA double-strand break repair in human glioma cells. *Cancer Biol. Ther.* **8**, 730–738 (2009).
45. Wei, F. et al. Inhibition of ERK activation enhances the repair of double-stranded breaks via non-homologous end joining by increasing DNA-PKcs activation. *Biochim. Biophys. Acta* **1833**, 90–100 (2013).
46. Hensch, N. R. et al. Sensitization to Ionizing Radiation by MEK Inhibition Is Dependent on SNAI2 in Fusion-Negative Rhabdomyosarcoma. *Mol. Cancer Ther.* **22**, 123–134 (2023).
47. Vellano, C. P. et al. Androgen receptor blockade promotes response to BRAF/MEK-targeted therapy. *Nature* **606**, 797–803 (2022).
48. Peterziel, H. et al. Rapid signalling by androgen receptor in prostate cancer cells. *Oncogene* **18**, 6322–6329 (1999).
49. Liao, R. S. et al. Androgen receptor-mediated non-genomic regulation of prostate cancer cell proliferation. *Transl. Androl. Urol.* **2**, 187–196 (2013).
50. Chia, K. M., Liu, J., Francis, G. D. & Naderi, A. A feedback loop between androgen receptor and ERK signaling in estrogen receptor-negative breast cancer. *Neoplasia* **13**, 154–166 (2011).
51. Naderi, A., Chia, K. M. & Liu, J. Synergy between inhibitors of androgen receptor and MEK has therapeutic implications in estrogen receptor-negative breast cancer. *Breast Cancer Res* 13, (2011).
52. Baumgartner, M., Drake, K. & Kanadia, R. N. An Integrated Model of Minor Intron Emergence and Conservation. *Front Genet* **10**, 473149 (2019).
53. Tanikawa, M., Sanjiv, K., Helleday, T., Herr, P. & Mortusewicz, O. The spliceosome U2 snRNP factors promote genome stability through distinct mechanisms; transcription of repair factors and R-loop processing. *Oncogenesis* **5**, e280–e280 (2016).
54. Lai, J. J. et al. Androgen receptor influences on body defense system via modulation of innate and adaptive immune systems: lessons from conditional AR knockout mice. *Am. J. Pathol.* **181**, 1504–1512 (2012).
55. Guan, X. et al. Androgen receptor activity in T cells limits checkpoint blockade efficacy. *Nature* **606**, 791–796 (2022).
56. Kim, D., Paggi, J. M., Park, C., Bennett, C. & Salzberg, S. L. Graph-based genome alignment and genotyping with HISAT2 and HISAT-genotype. *Nat. Biotechnol.* **37**, 907–915 (2019).
57. Cunningham, F. et al. Ensembl 2022. *Nucleic Acids Res* **50**, D988–D995 (2022).
58. Putri, G. H., Anders, S., Pyl, P. T., Pimanda, J. E. & Zanini, F. Analysing high-throughput sequencing data in Python with HTSeq 2.0. *Bioinformatics* **38**, 2943–2945 (2022).
59. Love, M. I., Huber, W. & Anders, S. Moderated estimation of fold change and dispersion for RNA-seq data with DESeq2. *Genome Biol.* **15**, 1–21 (2014).
60. Hu, J. et al. Non-parametric quantification of protein lysate arrays. *Bioinformatics* **23**, 1986–1994 (2007).
61. Brady, D. C. et al. Copper is required for oncogenic BRAF signalling and tumorigenesis. *Nature* **509**, 492–496 (2014).
62. Michmerhuizen, A. R. et al. Estrogen receptor inhibition mediates radiosensitization of ER-positive breast cancer models. *npj Breast Cancer* **8**, 1–12 (2022).
63. Pesch, A. M. et al. Short-term CDK4/6 inhibition radiosensitizes estrogen receptor-positive breast cancers. *Clin. Cancer Res.* **26**, 6568–6580 (2020).

Acknowledgements

The authors thank Drs. Arul Chinnaiyan and Abhijit Parolia for providing the R1881, the Advanced Genomics Core at the University of Michigan for library preparation and RNA-sequencing, and Advaita Bioinformatics for the use of analysis software for RNA-sequencing results. This research was funded by NCI grant 5R21CA267147-02 to C.W.S. and L.J.P., a Breast Cancer

Research Foundation (BCRF) Grant to L.J.P. (BCRF-21-128). A.R.M., and A.M.P. were supported by National Institute of General Medical Sciences (NIGMS) training grants: T32-GM113900 (A.R.M.), T32-GM007315 (A.R.M.), T32-GM007767 (A.M.P.). B.M. was supported by a National Human Genome Research Institute (NHGRI) training grant: T32-HG000040. A.M.P. was supported by a Ruth L. Kirschstein NRSA F31 award (F31CA254138). A.R.M. was supported by the Rackham Predoctoral Fellowship Program. This work was also supported by Rackham Graduate School Research Grants (A.R.M., B.M.).

Author contributions

Concept and design: B.M., B.H., A.R.M. Acquisition, analysis, or interpretation of data: B.M., B.H., A.R.M., B.C.C., A.M.P., L.M.L., D.G., C.W., P.R., R.A.Z., V.M., M.T., E.H., K.M.J., S.T., M.L., D.E.S., A.P.B., L.J.P., C.W.S. Drafting of manuscript: B.M., B.H., A.R.M., C.W.S. Statistical analysis: B.M., B.H., A.R.M. Supervision: D.E.S., A.P.B., L.J.P., C.W.S.

Competing interests

L.J.P. is a paid consultant for UpToDate. The funders had no role in the design of the study; in the collection, analyses, or interpretation of data; in the writing of the manuscript; or in the decision to publish the results.

Additional information

Supplementary information The online version contains supplementary material available at https://doi.org/10.1038/s41523-026-00916-1.

Correspondence \and requests for materials should be addressed to Corey W. Speers.